The Histrionicotoxin-Sensitive Ethidium Binding Site Is Located Outside of the Transmembrane Domain of the Nicotinic Acetylcholine Receptor: A Fluorescence Study†

David A. Johnson*,§ and John M. Nuss‡,∥

Division of Biomedical Sciences and Departments of Neuroscience and Chemistry, University of California, Riverside, California 92521-0121

Received March 3, 1994; Revised Manuscript Received May 9, 1994®

ABSTRACT: A novel, relatively photostable, long-wavelength fluorescent membrane probe, *N*-(Texas Red sulfonyl)-5(and 6)-dodecanoylamine (C_{12}-Texas Red), was synthesized and used as an electronic energy acceptor for Förster fluorescence resonance energy transfer (FRET) between ethidium bound to a histrionicotoxin-sensitive binding site on the *Torpedo* nicotinic acetylcholine receptor (AChR) and the lipid membrane surface. FRET from membrane-partitioned 5-(*N*-dodecanoylamino)fluorescein (C_{12}-fluorescein) to the membrane-partitioned C_{12}-Texas Red was also determined with a parallel set of cuvettes to (1) compare FRET results with a donor in a known position in the membrane and (2) assess the surface density of the membrane-partitioned C_{12}-Texas Red. Stern–Volmer analysis of the FRET results showed that C_{12}-Texas Red quenched membrane-partitioned C_{12}-fluorescein fluorescence 2.9 times more effectively than it quenched the receptor-bound ethidium fluorescence even though the Förster critical distances for the two donor-acceptor pairs were very similar (49.9 and 54.3 Å, respectively). Analysis of the ethidium to C_{12}-Texas Red FRET as a function of acceptor surface density with the assumptions that the donor is attached along the major axis of symmetry of a cylindrical protein embedded perpendicularly into the membrane (On-Axis FRET model) suggested that the distance of closest approach between the receptor-bound ethidium and the membrane surface was ~52 Å. Because the minimum distance between the surface of the lipid-membrane domain and the major symmetry axis of the AChR is ~28 Å, the FRET results strongly suggest that the ethidium binding site is not located near the entrance of the luminal transmembrane domain is generally assumed. These results for the first time provide direct evidence for an histrionicotoxin-sensitive NCI binding site that is located outside the transmembrane domain of the desensitized nicotinic acetylcholine receptor.

Noncompetitive inhibitors (NCIs)[1] of the muscle-type nicotinic acetylcholine receptor (AChR) block agonist-induced cation fluxes without impeding agonist binding—indeed, most NCIs enhance agonist binding (Léna & Changeux, 1993). NCIs can potentially interact with at least two classes of binding sites: histrionicotoxin (HTX)-sensitive and -insensitive (Heidmann *et al.*, 1983). The HTX-sensitive sites are associated with a binding stoichiometry of one NCI molecule/functional AChR unit. Agents that bind to the HTX-sensitive class of sites are structurally heterogeneous and include ethidium (Herz *et al.*, 1987), quinacrine (Adams, 1981), phencyclidine (PCP) (Albuquerque *et al.*, 1980), meproadifen (Krodel *et al.*, 1979), and, of course, HTX (Eldefrawi *et al.*, 1978). Because most agents that interact with the HTX-sensitive sites also interact with the HTX-insensitive sites, albeit with a substantially lower affinity, the agents that bind to the HTX-sensitive sites are often called high-affinity NCIs.

Despite the fact that high-affinity NCIs bind with a unitary stoichiometry, there is a growing body of evidence for the existence of more than one HTX-sensitive binding site on the receptor (Taylor *et al.*, 1991). The binding of high-affinity NCIs at one HTX-sensitive site thus precludes simultaneous binding of NCIs at other sites. The best characterized binding site appears to be formed by two homologous hydroxylated amino acids in the M2 transmembrane segments that are located about two-thirds the way down the transmembrane region (from the extracellular side) of the AChR (Galzi *et al.*, 1991). An NCI binding site may exist a few amino acid residues above this site (White & Cohen, 1992). Another HTX-sensitive NCI binding site may be located at the extracellular entrance to the transmembrane luminal domain of the AChR, because [^{3}H]meproadifen mustard affinity labels a side chain in the extracellular loop between M2 and M3 transmembrane segments of the α-subunit (αGlu^{262}) (Dreyer *et al.*, 1986; Pedersen *et al.*, 1990). Quinacrine, moreover, may bind to an additional site, because [^{3}H]quinacrine azide photoaffinity-labels the beginning of the extracellular end of the M1 transmembrane segment of the α-subunit (αArg^{209} and αPro^{211}) (Karlin, 1991). It has been postulated that this site is localized outside the lumen at a lipid–protein interface of the desensitized AChR, because PCP- and HTX-sensitive quinacrine fluorescence is very susceptible to quenching by lipophilic spin and fluorescent probes in the presence of an agonist (Valenzuela *et al.*, 1992b; Arias *et al.*, 1993a,b).

† This work was supported by NSF Grant IBN-9215105 to D.A.J.

* Corresponding author: David A. Johnson, Ph.D., Division of Biomedical Sciences, University of California, Riverside, CA 92521-0121. Phone no. (909) 787-3831. FAX no. (909) 787-5504.

§ Division of Biomedical Sciences and Department of Neuroscience.

‡ Department of Chemistry.

∥ Present address: Chiron Corp., 4560 Horton St., Emeryville, CA 94608-2916.

® Abstract published in *Advance ACS Abstracts,* July 15, 1994.

[1] Abbreviations and trivial names: AChR, nicotinic acetylcholine receptor; ACh, acetylcholine; buffer I, 100 mM NaCl and 10 mM sodium phosphate, pH 7.4; C_{12}-fluorescein, 5-(*N*-dodecanoylamino)fluorescein; C_{12}-Texas Red, *N*-(Texas Red sulfonyl)-5(and 6)-dodecanoylamine; dansylethyltrimethylammonium, [1-(dimethylamino)naphthalene-5-sulfonamido]ethyltrimethylammonium perchlorate; FRET, Förster fluorescence resonance energy transfer; HTX, histrionicotoxin; NCI, noncompetitive inhibitor; PCP, phencyclidine.

0006-2960/94/0433-9070$04.50/0

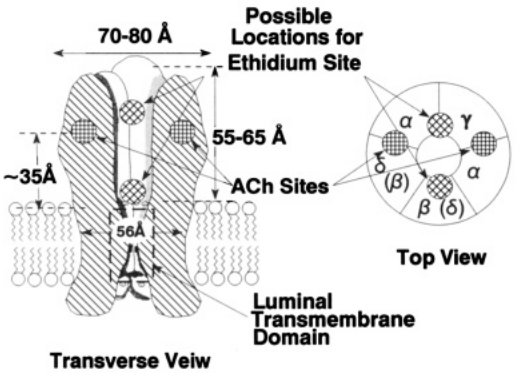

FIGURE 1: Model of the AChR. Left panel: Transverse schematic representation of the AChR (following Unwin, 1993) showing the possible locations of the ethidium binding site. Right panel: Representation of the top view of the AChR showing the relative positions of the two ACh binding sites and possible locations of the ethidium binding site relative to the various AChR subunits.

Largely because ethidium is a high-affinity NCI that binds in a hydrophobic pocket (Herz *et al.*, 1987) within 20–40 Å from the acetylcholine (ACh) binding sites (Herz *et al.*, 1989), which appear to be located about 35 Å above the membrane surface (Valenzuela *et al.*, 1994), it has been postulated that ethidium binds near the entrance of the luminal transmembrane domain of the receptor (Herz *et al.*, 1989; Herz *et al.*, 1991; Herz & Atherton, 1992). However, these observations are also consistent with ethidium binding in a hydrophobic pocket at about the level of and between the two ACh binding sites on the doughnut-shaped extracellular domain of the receptor (Figure 1). To distinguish between these possibilities, we used Förster fluorescence resonance energy transfer (FRET) techniques to measure the minimum distance between the receptor-bound ethidium and the lipid membrane surface. Geometrical considerations show that, if ethidium is binding near the extracellular entrance to the luminal transmembrane domain, then the minimum distance between the AChR-bound ethidium and the surface of the lipid membrane would be <28 Å, whereas, a much greater distance would be expected if it were located near the level of the ACh binding sites. To measure FRET between AChR-bound ethidium and the lipid membrane surface, a novel and relatively photostable, long-wavelength fluorescent lipophilic probe, *N*-(Texas Red sulfonyl)-5(and 6)-dodecanoylamine (C_{12}-Texas Red), was synthesized and used as an electronic energy acceptor for receptor-bound ethidium. C_{12}-Texas Red is composed of a charged fluorophore attached to a hydrocarbon membrane anchor. With such a molecular configuration this probe would be expected to position itself at the water–lipid interface and permit distance measurements between the ethidium binding site and the lipid membrane surface. We found that, consistent with an extraluminal location, receptor-bound ethidium was substantially more (~46 Å) than 28 Å from the lipid membrane surface.

EXPERIMENTAL PROCEDURES

Materials. 5-(*N*-Dodecanoylamino)fluorescein (C_{12}-fluorescein), 5- and 12-doxylstearate, and Texas Red sulfonyl chloride were purchased from Molecular Probes (Eugene, OR). *Torpedo californica* electric rays were obtained from Marinus Inc. (Long Beach, CA). Phencyclidine (PCP), carbamylcholine, and suberyldicholine were purchased from Sigma (St. Louis, MO). [1-(Dimethylamino)naphthalene-5-sulfonamido]ethyltrimethylammonium perchlorate (dansylethyltrimethylammonium) was acquired from Pierce Chemical Co. (Rockford, IL).

Receptor Isolation. Base-treated nicotinic acetylcholine receptor-enriched membranes, designated below as AChR membranes, were isolated from the *Torpedo californica* electric organ with previously described procedures (Johnson & Yguerabide, 1985). The receptor-specific activities were determined by the reduction of dansylethyltrimethylammonium (6.6 μM) fluorescence produced by the titration of suberyldicholine into AChR-associated membrane suspensions (0.3 mg of protein/mL) in the presence of PCP (100 μM), following a modification of the method of Neubig & Cohen (1979). The receptor specific activities ranged between 1.1 and 1.8 nmol of suberyldicholine binding sites/mg of protein.

Synthesis of C_{12}-Texas Red. Dodecylamine (5.4 μmol) was added to a sealed flask containing Texas Red sulfonyl chloride (16 μmol) dissolved in 2 mL of acetonitrile. The reaction mixture was incubated for 5 h at room temperature before it was rotary evaporated and applied to a silica gel flash chromatography column (EM Merck, 230–400 mesh) equilibrated with a 20:1 (v/v) mixture of methylene chloride and methanol. The eluted fractions that contained C_{12}-Texas Red were rotary evaporated. Silica gel thin-layer chromatography with methylene chloride–methanol (9:1, v/v) as the mobile phase showed a single spot with an R_f value of 0.42. Although the spectra were very complex. ^{1}H- and ^{13}C-NMR analysis of the C_{12}-Texas Red showed the presence of two isomeric C_{12}-Texas Red sulfonamides (*N*-(Texas Red sulfonyl)-5(and 6)dodecanoylamine). The ^{13}C NMR showed two compounds each having 31 signals, as expected for these adducts. The high-resolution mass spectrum confirmed this assignment, as chemical ionization mass spectroscopy (NH_3 used as the reagent gas) gave the $(M + H)^+$ peak as 772.3487 (expected for $C_{43}H_{54}N_3O_6S_2$ is 772.3457); the actual molecular formula of the adducts is $C_{43}H_{53}N_3O_6S_2$).

Fluorescence Measurements. Steady-state fluorescence measurements were made with a Fluoromax spectrofluorometer (Spex Industries, Edison, NJ).

Doxylstearate Quenching of Membrane-Partitioned C_{12}-Texas Red Fluorescence. The relative concentrations of the stock doxylstearate solutions and the doxylstearate quenching of membrane-partitioned C_{12}-Texas Red fluorescence were performed via procedures described elsewhere (Arias *et al.*, 1993a). Excitation and emission wavelengths were 580 and 610 nm, respectively. Also, to reduce stray-light effects a 580-nm Oriel narrow-band interference filter and a Corning 2–63 cut-off filter were placed in the paths of the excitation and emission beams, respectively.

The previously determined (Arias *et al.*, 1993a) values for the fractional partitioning of 5-doxylstearate (0.96) and 12-doxylstearate (0.79) into the AChR membranes were multiplied by the total concentration of *n*-doxylstearate in each sample cuvette to determine the relative concentration of each spin label in the membrane.

Quantum Yield of Receptor-Bound Ethidium. The fluorescence quantum yield of receptor-bound ethidium (Q_D) was determined in two steps. First, by using the ratio method of Chen (1965) with fluorescein in 0.1 N NaOH as a standard (Q = 0.85) (Parker & Rees, 1960) the quantum yield of ethidium in buffer I was determined to be 0.028. Second, because the quantum yield of ethidium is essentially proportional to its fluorescent lifetime (Olmstead & Kearns, 1977), the receptor-bound quantum yield of ethidium was calculated by multiplication of the quantum yield of ethidium in buffer I by the ratio of the fluorescence lifetime of receptor-bound to free ethidium in buffer I ($\tau_B/\tau_F = 13.1$) (Herz *et al.*, 1987).

Fractional Specific Ethidium Binding to the AChR Membranes. Ethidium (3 μM) and AChR membranes (1 μM in suberyldicholine binding sites) were suspended in 0.1 mL of buffer I and carbamylcholine (1 mM) ± PCP (100 μM). (Excess carbamylcholine was added to all cuvettes containing ethidium to prevent ethidium from binding to the ACh sites and to convert the receptor into a state that is associated with a high-affinity HTX-sensitive ethidium binding.) Parallel samples, which contained equivalent concentrations of ethidium in buffer I or AChR membranes suspended in buffer I, both in the presence of carbamylcholine, were used to determine the total and background fluorescence, respectively. The samples were centrifuged with a Beckman Airfuge at 30 psi (178000g) for 10 min at room temperature, the supernatants were placed in Ultra-micro cuvettes (catalog no. 105.251-QS, Hellma GmBH & Co, Forest Hills, NY), and the ethidium emission was monitored at 580 nm with excitation at 530 nm.

The fraction (f_B) of the total added ethidium that specifically binds to a PCP-sensitive site was calculated with the expression

$$f_B \frac{I_{total} - I^S_{minus\ PCP}(1 + K_P^*)}{I_{total}} = \frac{L_B}{L_T} \quad (1)$$

where $I^S_{minus\ PCP}$ is the background-subtracted supernatant fluorescence of the samples that contained both fluorophore and AChR membranes but not PCP. K_P^* is the apparent membrane-partition coefficient for ethidium and was determined following the procedures described elsewhere for dansyl-C_6-choline (Valenzuela *et al.*, 1994). L_B and L_T are the amounts of specifically bound and total ligand, respectively.

Surface Density of C_{12}-Texas Red. Acceptor surface density was assessed by measuring the ability of C_{12}-Texas Red to quench the emission of C_{12}-fluorescein (0.4 μM) previously incorporated (2 h) into the AChR membranes (1 μM in suberyldicholine binding sites). Both C_{12}-Texas Red and C_{12}-fluorescein would be expected to be interdigitated into the same domains and could come within a van der Waals distance of each other, i.e., a distance of closest approach about equal to zero. By comparing the observed quenching efficiency of this donor–acceptor pair with the theoretical relation between quenching efficiency and surface density (Fung & Stryer, 1978), estimates of lipid probe surface densities were made for each AChR-membrane preparation studied. All samples were suspended in 10 mM sodium phosphate buffer, pH 7.4, in the presence of 1 M NaCl to minimize charge effects between the donors and acceptors.

The surface density of acceptors at each step of the titration was estimated by initially solving numerically the equations for donors and acceptors randomly distributed in a planar–lipid membrane (which is equivalent to eqs A4–A6) for incremental values of σR_0^2 with the distance of closest approach set at 0 Å and R_0 at 49.9 Å, the calculated Förster critical distance for C_{12}-fluorescein/C_{12}-Texas Red donor–acceptor pair. The resultant calculated values of I_{DA}/I_D vs σR_0^2 were fit to a binomial function $[I_{DA}/I_D = a(\sigma R_0^2)^b + c(\sigma R_0^2)^d + e]$ from which the observed I_{DA}/I_D ratios for each AChR membrane preparation could be related to estimated values for σR_0^2 for each amount of added acceptor.

FRET Measurements. Ethidium (3 μM), carbamylcholine (1 mM), and AChR membranes (1 μM in suberyldicholine binding sites) were suspended in buffer I in the presence and absence of PCP (100 μM). The excess carbamylcholine was added to prevent ethidium from binding to the acetylcholine binding sites and thus increasing the specificity of the ethidium binding. A parallel cuvette that contained the carbamylcholine, PCP, and AChR membranes was used to estimate the intrinsic fluorescence of the acceptor and background fluorescence. The C_{12}-Texas Red was dissolved in dimethyl sulfoxide (which had no measurable effect on ethidium fluorescence) and was added to the cuvettes with a Hamilton syringe. After each titrant addition, the samples were incubated for 15 min prior to the fluorescence measurements.

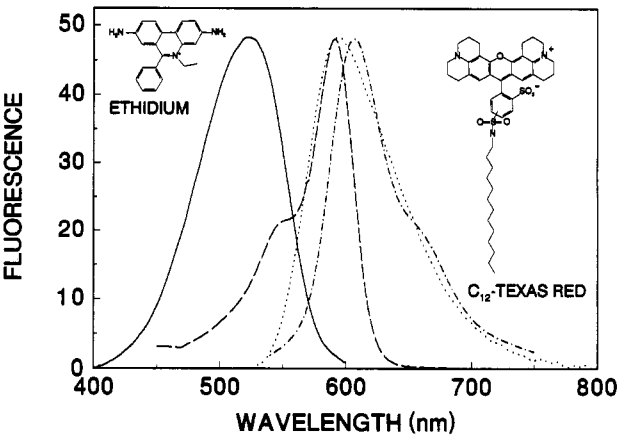

FIGURE 2: Spectral overlap between receptor-bound ethidium (donor) and membrane-partitioned C_{12}-Texas Red (acceptor). Shown are the corrected excitation (dashed line) and emission (dot/dashed line) spectra of C_{12}-Texas Red (0.4 μM) partitioned into AChR membrane fragments (1.0 μM in suberyldicholine binding sites) in buffer I. The corrected difference excitation (solid line) and emission (dotted line) spectra of ethidium (3 μM) in a suspension of AChR membranes (1.0 μM in suberyldicholine binding sites) preincubated with carbamylcholine (1 mM) were produced by subtracting the spectra taken of samples that did not contain PCP from spectra taken of samples that did contain PCP (0.1 mM). The peak excitation and emission wavelengths of membrane-partitioned C_{12}-Texas Red were 591 and 608 nm, respectively.

Because only a fraction of the total added ethidium (f_B = 0.17–0.20, depending on the AChR membrane preparation) was specifically bound to the ACh binding sites, the determination of the specific FRET to the membrane-partitioned acceptors required separation of the bound-donor fluorescence (I_B) from the free and nonspecifically membrane-partitioned donor fluorescence. This was accomplished by using eq 2

$$I_B = I_{minus\ PCP} - (1 - f_B)I_{plus\ PCP} \quad (2)$$

where $I_{minus\ PCP}$ and $I_{plus\ PCP}$ are the magnitudes of fluorescence of samples that did not or did contain PCP, respectively. (Although eq 2 was originally derived (Valenzuela *et al.*, 1994) with the assumption that fluorophore absorbance is unaffected by binding, the equation turns out to be still valid if the absorbance changes upon binding or membrane partitioning.) The observed fluorescence was corrected for dilution and inner filter effects of the acceptor. The fraction of ethidium that was not bound to its PCP-sensitive binding site ($1 - f_B$) was determined while the centrifugation assay described elsewhere (Valenzuela *et al.*, 1994).

RESULTS

Spectral Characterization and FRET Parameters. The corrected excitation and emission difference spectra (PCP-sensitive) of AChR-bound ethidium and the excitation and emission spectra of C_{12}-Texas Red partitioned into the AChR membranes are shown in Figure 2. As previously reported (Herz *et al.*, 1987; Valenzuela *et al.*, 1992a), the PCP-sensitive ethidium difference spectra displays excitation and emission

Table 1: Summary of FRET Parameters for Excitation Energy Transfer from Receptor-Bound Ethidium or Membrane-Partitioned C_{12}-Fluorescein to Membrane-Partitioned C_{12}-Texas Red

donor	Q_D[a]	J[b] (cm^3/M)	R_o[c] (Å)
AChR-bound ethidium	0.37[d]	4.54×10^{-13}	54.3
membrane-partitioned C_{12}-fluorescein	0.34[e]	3.01×10^{-13}	49.9

[a] Donor quantum yield. [b] Overlap integral calculated as described in the Experimental Procedures. [c] Förster critical distance calculated as described in the Experimental Procedures. [d] Determined by multiplying the quantum yield of ethidium in buffer (0.028) by the enhancement of the fluorescence lifetime of ethidium upon specifically binding to the AChR (13.1). [e] From Holowka & Baird, 1983.

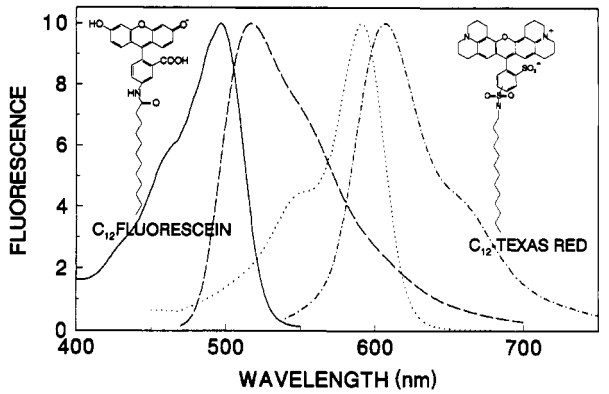

FIGURE 3: Spectral overlap of membrane-partitioned C_{12}-fluorescein (donor) and C_{12}-Texas Red (acceptor). Shown are the corrected excitation (solid line) and emission (dashed line) spectra of C_{12}-fluorescein (0.4 μM) and the corrected excitation (dotted line) and emission (dot/dashed line) of membrane-partitioned C_{12}-Texas Red into AChR membrane fragments (1.0 μM in suberyldicholine binding sites).

maxima at about 522 and 595 nm, respectively. The excitation and emission spectra of membrane-partitioned C_{12}-Texas Red, relative to what is typically observed with Texas Red–protein conjugates (Johnson *et al.*, 1993), are somewhat red (4 nm) and blue (10 nm) shifted, respectively. The corrected excitation and emission maxima of membrane-partitioned C_{12}-Texas Red were 591 and 609 nm, respectively.

Because the samples of the membrane-partitioned C_{12}-Texas Red are turbid, it was not possible to directly measure its absorption spectrum. Consequently, the excitation spectrum of membrane-partitioned C_{12}-Texas Red was measured; its maximum molar extinction was assumed to be 85 000 M^{-1} cm^{-1} (Haugland, 1992), and its absorption spectrum was assumed to mirror the spectral profile of its excitation spectrum. The overlap integral between the emission spectrum of receptor-bound ethidium and the inferred absorption spectrum of membrane-partitioned C_{12}-Texas Red was calculated (eq A3) to be 4.54×10^{-13} cm^3/M (Table 1). Using a value of 0.37 for the quantum yield (Q_D) of receptor-bound ethidium and a value of $^2/_3$ for the orientation factor (κ^2), the Förster critical distance (R_o) for ethidium/C_{12}-Texas Red donor–acceptor pair was calculated (eq A2) to be 54.3 Å (Table 1).

The corrected excitation and emission spectra of C_{12}-fluorescein and C_{12}-Texas Red partitioned into AChR membranes are shown in Figure 3. Again, assuming that the maximum molar extinction of C_{12}-Texas Red is 85 000 M^{-1} cm^{-1} (Haugland, 1992), the overlap integral between the emission spectrum of C_{12}-fluorescein and the inferred absorption spectrum of membrane-partitioned C_{12}-Texas Red was calculated (eq A3) to be 3.01×10^{-13} cm^3/M (Table 1). Using a value of 0.34 for the quantum yield of C_{12}-fluorescein (Holowka & Baird, 1983), the Förster critical distance was calculated (eq A2) to be 49.9 Å (Table 1).

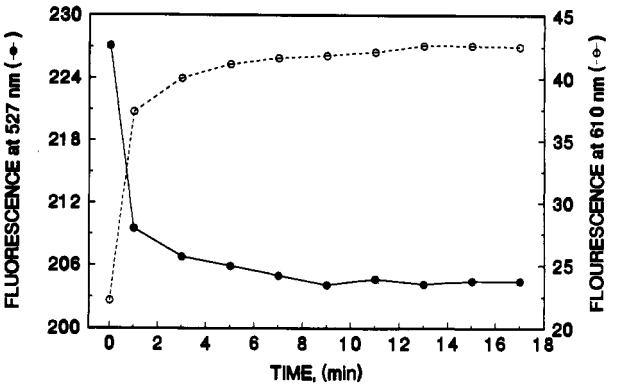

FIGURE 4: Time-dependent partitioning of C_{12}-Texas Red into AChR membrane fragments. The quenching of C_{12}-fluorescein fluorescence (emission at 527 nm; filled circles) and concomitant sensitization of C_{12}-Texas Red fluorescence (emission at 610 nm; unfilled circles) were monitored from emission spectra (excitation at 480 nm) taken at 1-min intervals after C_{12}-Texas Red (0.3 μM) was added to AChR membrane fragments (1.0 μM in suberyldicholine binding sites) containing membrane-partitioned C_{12}-fluorescein (0.4 μM). A Corning 3–70 cut-off filter was placed in the path of the emission beam to reduce stray light effects.

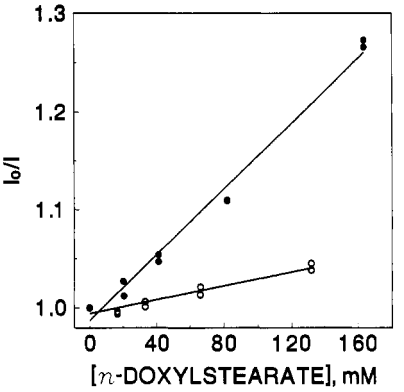

FIGURE 5: *n*-Doxylstearate quenching of membrane-partitioned C_{12}-Texas Red fluorescence. The results represent the fluorescence in the absence (I_o) divided by in the presence (I) of various concentrations of either 5-doxylstearate (filled circles) or 12-doxylstearate (open circles). Fluorescence from the C_{12}-Texas Red (0.6 μM) partitioned into AChR membranes (1.0 μM in suberyldicholine binding sites).

Time Course of C_{12}-Texas Red Partitioning. To determine the time required for C_{12}-Texas Red incorporation into the AChR membranes and therefore the minimum incubation time between each step of the FRET titrations, the time course of C_{12}-Texas Red partitioning was measured. Both donor quenching and concomitant acceptor sensitization were monitored after C_{12}-Texas Red was added to suspensions of AChR membranes containing C_{12}-fluorescein. Figure 4 shows that after ~10 min donor quenching and acceptor sensitization had reached equilibrium, indicating maximum C_{12}-Texas Red partitioning. Hence, for each step of the FRET titrations described below, fluorescence measurements were taken at least 15 min after the C_{12}-Texas Red was added.

Doxylstearate Quenching of Membrane-Partitioned C_{12}-Texas Red. To partially assess the transverse location of C_{12}-Texas Red in the AChR membranes, the relative efficiencies of the 5-doxylstearate or 12-doxylstearate to quench the fluorescence of membrane-partitioned C_{12}-Texas Red were also measured. The C_{12}-Texas Red is composed of a charged fluorophore and a hydrophobic 12-carbon chain. The I_o/I vs *n*-doxylstearate concentration plots are shown in Figure 5. The 5-doxylstearate displayed about 5 times the quenching efficacy of the 12-doxylstearate isomer. Because the nitroxide

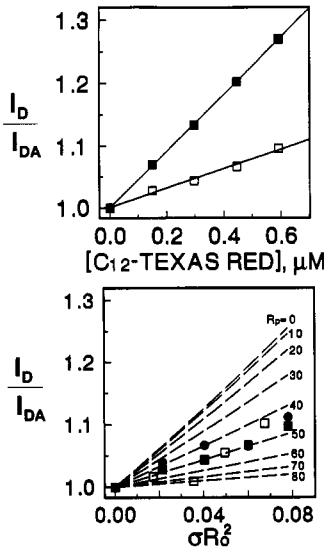

FIGURE 6: FRET between two donors, receptor-bound ethidium and membrane-partitioned C_{12}-fluorescein, and membrane-partitioned C_{12}-Texas Red. Upper panel: Corrected receptor-bound ethidium (filled squares) and membrane-partitioned C_{12}-fluorescein (unfilled squares) fluorescence from a single experiment plotted as the ratio of emission in the absence divided by the presence of acceptor, C_{12}-Texas Red (I_D/I_{DA}). Lower panel: Plotted as points (different point symbols for each of three determinations) are the ratios of AChR-bound receptor-bound ethidium (donor) fluorescence, in the absence (I_D) and in the presence (I_{DA}) of the membrane-partitioned C_{12}-Texas Red (acceptor) as a function of the surface density of acceptors (σ) times the R_o^2. Plotted as a series of dashed lines are the calculated relation between I_D/I_{DA} and σR_o^2 by using the Off-Axis FRET model for discrete donors attached at a distance δ from the major symmetry axis of a cylindrical protein embedded perpendicularly into a planar membrane in which acceptors are randomly distributed. Calculations were made and plotted for various transverse distances (R_P) between the donors and membrane surface using eqs A6–A11 (α = 28 Å; δ = 20 Å). The surface density of acceptors (σR_o^2) was determined as described in the Experimental Procedures.

moiety of the membrane-partitioned 5-doxylstearate has been shown to be positioned closer to the water–lipid interface than the nitroxide moiety of the 12-doxylstearate (Marsh & Barrantes, 1978), the greater ability of the 5-doxylstearate to quench C_{12}-Texas Red fluorescence indicates that the fluorescent moiety in the C_{12}-Texas Red is closer to the 5-doxyl group than the 12-doxyl group and is therefore closer to the water–lipid interface.

FRET Measurements. The ability of membrane-partitioned C_{12}-Texas Red to quench the emission from specifically-bound ethidium and membrane-partitioned C_{12}-fluorescein was initially compared by plotting the specific emission of each energy donor in the absence (I_D) divided by the presence of (I_{DA}) of various concentrations of C_{12}-Texas Red (Figure 6). Plotted in this way specific C_{12}-fluorescein emission was 2.9-fold more effectively quenched than the emission from specifically bound ethidium (Figure 6, upper panel). This type of plot only provides a semiquantitative comparison, because (1) the surface density of C_{12}-Texas Red varies with each AChR-membrane preparation and (2) the plot does not correct for the differences in the Förster critical distances (R_o) associated with each donor-acceptor pair.

To deal with these problems, the C_{12}-Texas Red/C_{12}-fluorescein quenching data was used to estimate the surface density (σ) of C_{12}-Texas Red for each titration step with each AChR membrane preparation, and the ethidium quenching results (I_D/I_{DA}) from the different membrane preparations were plotted as a function of σR_o^2 (Figure 6, lower panel). Because it has been frequently assumed that ethidium binds in the lumen of the receptor at the level of the water–lipid interface (Herz *et al.*, 1989; Arias *et al.*, 1993b), the ethidium/C_{12}-Texas Red FRET results (Figure 6, lower panel) were initially compared with theoretical plots (I_D/I_{DA} vs σR^2) for an On-Axis FRET model (Appendix). The On-Axis FRET model assumes that the donor is attached along the major symmetry axis of cylindrical proteins that are embedded perpendicularly into a planar membrane and the acceptor groups are randomly distributed on the surface of the membrane. This analysis (results not shown) suggested that the observed ethidium-to-Texas Red FRET was of a magnitude consistent with about a 52-Å minimum distance between the receptor-bound ethidium and the membrane-partitioned C_{12}-Texas Red.

Given the cross-sectional radius (~28 Å) and thickness (20–30 Å) of the transmembrane region of the intact receptor (Toyoshima & Unwin, 1990), a 52-Å minimum distance would be incompatible with ethidium binding to the receptor either at the level of the water–lipid interface or in the transmembrane domain. For receptor-bound ethidium to be positioned along the major symmetry axis of the AChR, ~52 Å from the surface of the lipid membrane and within 20–40 Å from the ACh binding sites, ethidium would have to be positioned in about the center of the vestibule and not in contact with the receptor—an impossibility. Consequently, the ethidium FRET results were compared with theoretical plots that utilized the more complex Off-Axis model for protein-to-lipid FRET. (The Off-Axis model (Yguerabide, 1994) is similar to the On-Axis model except that the donors are assumed to be attached at a distance δ from the major axis of symmetry of the cylindrical proteins (Appendix).) This more complex model allows ethidium to be binding to the walls of the channel, 15–40 Å from the major symmetry axis. Because (1) receptor-bound ethidium (diameter ~10 Å) is inaccessible to polar solutes and must be sandwiched between hydrophobic peptidyl elements of the AChR (Herz & Atherton, 1992; Arias *et al.*, 1993b), (2) the inner diameter of the lumen of the extracellular domain of the receptor is 20–25 Å, and (3) the cross-sectional diameter of the transmembrane domain is ~56 Å (Unwin, 1993), α and δ were set at 20 and 28 Å, respectively. (α was set at 20 Å, because the radius of the cylindrically shaped vestibule is about 15 Å and ethidium binds to a hydrophobic pocket on the AChR). The equations for this more complex Off-Axis FRET model were solved numerically (eqs A6–A11) for various values of σR_o^2 and the transverse distance (R_P) from receptor-bound ethidium to the chromophore in C_{12}-Texas Red positioned at the water–lipid interface. These theoretical values are plotted as dashed lines in the lower panel of Figure 6. With the exception of one datum point, the observed FRET results lie between the 40- and 50-Å theoretical lines. Analysis of the slopes of the experimental data in relation to the theoretical lines yielded an R_P of ~46 Å. The disposition of nearly all of the data points between the 40- and 50-Å theoretical lines suggest an uncertainty in these results of at least ±5 Å.

Given the previously mentioned dimensions of the AChR, the observation that the acetylcholine binding sites are located ~35 Å above the water–lipid interface (Valenzuela *et al.*, 1994), and the distance between the ethidium and ACh binding sites (20–40 Å) (Herz *et al.*, 1989), the present results place the HTX-sensitive ethidium binding site well above the transmembrane domain and slightly above the level of the two acetylcholine binding sites in the extracellular domain.

DISCUSSION

During the past decade we have used quantitative fluorescence spectroscopy to map ligand binding sites on the AChR (Johnson *et al.*, 1984, 1990; Herz *et al.*, 1989; Valenzuela *et al.*, 1992b, 1994; Arias *et al.*, 1993a,b). Compared with X-ray crystallography and affinity labeling, fluorescence spectroscopy is a low-resolution technique that usually generates structural information in a piecemeal fashion. However, fluorescence spectroscopy has the advantages that the macromolecules under study do not have to be crystallized and information is generated about the intact macromolecules in their native state, without the necessity of reactive moieties near sites of interest. In the case of the ethidium binding site, we have previously shown that (1) lipophilic fluorescent and paramagnetic probes display limited accessibility to AChR-bound ethidium (Arias *et al.*, 1993b), (2) assuming that the distance between the ethidium binding site and the two ACh binding sites is about the same, then the ethidium binding site is 20–40 Å from each ACh binding site (Herz *et al.*, 1989), and (3) the ACh binding sites, which was in the extracellular domain, are ~35 Å from the lipid membrane surface (Valenzuela *et al.*, 1994).

Given the shape (doughnut) and dimensions (outer diameter = 70–80 Å, inner diameter 20–25 Å, height = 55–65 Å) of the extracellular domain (Unwin, 1993) and the fact that the two ACh binding site are 50–70 Å apart (Zingsheim *et al.*, 1982; Johnson *et al.*, 1984; Kubalek *et al.*, 1987) and ~35 Å above the lipid membrane surface (Valenzuela *et al.*, 1994) on the extracellular domain, the possible locations of the ethidium binding site are restricted to a zone that includes the entrance of the luminal transmembrane domain and a region between the two ACh binding sites. In this paper, we describe results that show that the minimum distance between the ethidium binding site and the surface of the lipid membrane domain is ~52 Å. Because the minimum distance between the lipid membrane domain and the major symmetry axis of the receptor is ~28 Å (transmembrane radius), these new findings are inconsistent with the entrance of the luminal transmembrane domain being the ethidium binding site and restrict its possible location to a zone ~46 Å above the membrane surface.

Relying on the observations (1) that the two ACh binding sites are located at the interfaces between the α–γ and α–δ subunits (Pedersen & Cohen, 1990; Czajkowski & Karlin, 1991; Czajkowski *et al.*, 1993) and (2) that the five subunits forming the receptor are probably arranged like barrel staves around the central channel of the receptor in either a α–γ–α–β–δ or α–γ–α–δ–β configuration (for a review see, Karlin, 1993) and assuming that the ethidium binding site is equidistant (20–40 Å) from the two ACh binding sites, approximate locations of the ethidium binding site can be deduced. Assuming an uncertainty of ±10 Å, the ethidium binding site would appear to be confined to a zone (36–56 Å above the membrane surface) that runs between the two ACh binding sites and includes either a portion of the β subunit or a region near the β–δ subunit interface (see Figure 1). Ethidium cannot be binding to the cytosolic side of the membrane, because its binding site is 20–40 Å from the ACh binding sites which are located on the extracellular domain about 35 Å above the lipid membrane surface (Valenzuela *et al.*, 1994). Wherever the ethidium binding site is located, it appears to be situated at a loci different from the transmembrane–NCI sites discussed in the introduction.

Both steric and allosteric models have been proposed to explain the ability of high-affinity NCIs to block the AChR in a mutually exclusive manner. However, with HTX-sensitive NCI binding sites located in luminal (Léna & Changeux, 1993) and possibly nonluminal (Valenzuela *et al.*, 1992b) transmembrane loci, as well as, in the distal portion of the extracellular domain (this paper), a simple steric or physical occlusion model for NCI action is inadequate to explain all the results. For high-affinity NCIs to act at separate sites at great distances from one another in a mutually exclusive manner, multiple binding site-specific conformations of the receptor must exist, particularly for those cases where physical occlusion cannot explain receptor blockade. Each binding site-specific conformation would allow a particular subclass of NCIs to bind to a distinct locus, to the exclusion of NCI binding to the other loci. This postulation would explain the unusual characteristics of NCIs, namely (1) their widely divergent structures extending from local anesthetics to quaternary cations, (2) their unitary binding stoichiometry, and (3) the multiplicity of NCI binding loci.

In light of this new information on the location of the ethidium binding site, it is of value to review our previous data on the location of the quinacrine binding site. We report that lipophilic paramagnetic probes display significantly greater accessibility to receptor-bound quinacrine than to receptor-bound ethidium (Arias *et al.*, 1993b). Because we assumed that ethidium binds near the entrance of the luminal transmembrane domain and that membrane-partitioned steroids and fatty acids cannot diffuse into the lumen, we concluded that the quinacrine binding site was not in the lumen of the receptor. If ethidium binds to a site at a distance from the transmembrane domain as shown in this paper, then it might be argued that quinacrine could be binding in the lumen of the AChR. But, for this to be true membrane-partitioned steroids and fatty acids must be able to diffuse into or very near the lumen. Blanton & Cohen (1992) have shown that photoactivated 1-azidopyrene (which is about the size, shape, and hydrophobicity of a steroid) labels the M1, M3, and M4 but not the luminal M2 transmembrane segments, which suggests limited accessibility of hydrophobic probes to the lumen. Thus, it seems probable that steroids and fatty acids are relative inaccessible to the lumen, and our previous postulation that quinacrine binds outside the lumen on the desensitized AChR remains valid.

Elsewhere we have discussed such issues as (1) the precision of transverse FRET measurements, (2) the validity of using a value of $^2/_3$ for the orientation factor (κ^2), and (3) the assumption that the membrane-partitioned acceptors are randomly distributed on the surface of the membrane (Azevedo & Johnson, 1990; Valenzuela *et al.*, 1994). With reference to this paper, an important issue is the uncertainty in the distance measurements. Primarily because of the potential nonrandom distribution of membrane acceptors, it is of value to measure FRET between a protein-bound donor and, at least, two membrane-partitioned acceptors in order to increase the precision of the calculated distances. It was not possible to use two membrane acceptors with the ethidium FRET studies described above because of the unavailability of photostable, long-wavelength membrane probes. We tried 1,1′-dioctadecyl-3,3,3′,3′-tetramethylindodicarbocyanine (Di-$IC_{18}(5)$) (data not shown) which emits at ~665 nm was found to be too unstable for the FRET experiments. We synthesized a C_{12}-carboxylnaphthofluorescein (data not shown) which emits at about 650 nm, but this was even more unstable than the $DiIC_{18}(5)$. In our previous effort to use FRET to measure the transverse distance between the ACh binding sites and the lipid membrane surface (Valenzuela *et al.*, 1994), the

calculated distances from two donor–acceptor pairs were within 9 Å of each other. It, therefore, seems that a conservative estimate of the uncertainty for the calculated transverse distance from the receptor-bound ethidium to the lipid membrane surface would be ±10 Å.

In conclusion, the results provide direct evidence for an HTX-sensitive NCI binding site that is located outside the transmembrane domain of the desensitized AChR. Specifically, the HTX-sensitive ethidium binding site on the muscle-type nicotinic acetylcholine receptor has been shown to be located ~46 Å above the lipid membrane surface. Combined with previous observations and with the assumption that the ACh binding sites are equidistant from receptor-bound ethidium, the present results further constrain the ethidium binding site to a zone that runs between the two ACh binding sites possibly near the α–γ subunit interface or on the β subunit. Moreover, with ethidium (diameter ~10 Å) embedded into the extracellular walls of the channel, where the opening is 20–25 Å in diameter, the possibility that ethidium could block agonist-induced ion fluxes by simple physical occlusion seems small, and therefore, ethidium appears to act allosterically to block AChR function.

ACKNOWLEDGMENT

We are grateful to Rebecca Wilson for assistance with the preparation of the AChR membranes.

APPENDIX

Fluorescence Resonance Energy Transfer (FRET) Models. The rate of excitation energy transfer (k_T) between discrete donors and suitable acceptors is related to the distance (r) separating the two molecules by eq A1 (Förster, 1959)

$$k_T = (1/\tau_D)(R_o/r)^6 \quad \text{(A1)}$$

where τ_D is the excited state lifetime of the donor in the absence of acceptor. R_o represents the Förster critical distance (in angstroms) and is defined by the expression

$$R_o = (9.765 \times 10^3)(\kappa^2 J Q_D n^{-4})^{1/6} \quad \text{(A2)}$$

The overlap integral, J (cm^6/mol), is calculated from the experimental spectra through the relationship

$$J = \sum I_D(\lambda)\epsilon_A(\lambda)\lambda^4\Delta\lambda/\omega I_D(\lambda)\Delta\lambda \quad \text{(A3)}$$

where $\epsilon_A(\lambda)$ is the molar extinction coefficient of the energy acceptor and $I_D(\lambda)$ is the relative donor emission spectrum, λ is the wavelength in centimeters, Q_D denotes the donor quantum yield in the absence of acceptor, and n represents the refractive index of the medium between donor and acceptor. For proteins the refractive index is about 1.4 (Stryer *et al.*, 1982), and κ^2 is the orientation factor and accounts for the relative orientation of the donor emission and acceptor absorption transition dipoles.

To translate the observed AChR-bound ethidium to membrane-partitioned C_{12}-Texas Red energy transfer data to intersite distances, two theoretical models were utilized: On-Axis and Off-Axis. The On-Axis model (Yguerabide, 1994) assumes that the donor and acceptor groups are randomly distributed in different planes in the same monolayer of the membrane. Also, the donor is assumed to be attached along the major symmetry axis of cylindrical proteins that are embedded perpendicularly into a planar membrane. The magnitude of FRET as a function of acceptor surface density for this On-Axis model can be numerically calculated by focusing on the time-resolved fluorescence decay of the donor

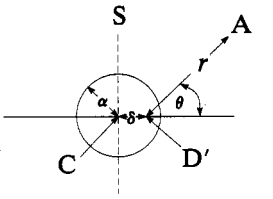

FIGURE 7: Schematic representation of the Off-Axis FRET model. Shown is a schematic representation in the acceptor plane of the coordinate system used to describe the position of an acceptor molecule A relative to the projection of the ethidium donor (D′) into the acceptor plane. The radius α of the circle is the distance of closest approach of lipid-embedded C_{12}-Texas Red acceptors to the center of the circle C. The center is the point where the transverse symmetry axis S of the cylindrically symmetric proteins intercept the acceptor plane. δ is the distance from the symmetry axis S at the center of the circle to D′. The position of A with respect to D′ in the acceptor plane is described by the distance r and angle θ.

with a fluorescence lifetime τ_D. The fluorescence intensity ($F(t)$) at any time t after excitation by a very short pulse of light is given by

$$F(t) = F(0)e^{-t/\tau_D}e^{-\sigma S(t)} \quad \text{(A4)}$$

$S(t)$, in turn, is defined by the integral

$$S(t) = \int_{r_c}^{\infty}[1 - e^{-(t/\tau_D)(R_o/r)^6}]2\pi r\, dr \quad \text{(A5)}$$

where $F(0)$ is the initial fluorescence intensity, σ is the surface density of energy acceptors, r is the distance between donor-acceptor pairs, and r_c is the minimum distance of approach between donors and acceptors. For steady-state emission, the ratio of donor fluorescence in the presence over absence of acceptor (I_D/I_{DA}) is given by the integral ratio

$$\frac{I_D}{I_{DA}} = \frac{\int_0^{\infty} F_D(t)\, dt}{\int_0^{\infty} F_{DA}(t)\, dt} \quad \text{(A6)}$$

where the subscripts D and DA denote the absence and presence of acceptor, respectively.

The Off-Axis model (Yguerabide, 1994) is similar to the On-Axis model except that the donors are assumed to be attached at a distance δ from the major axis of symmetry of the cylindrical proteins (Figure 7). The transverse distance from the protein-bound donor to acceptors positioned in the plane of the water-lipid interface is R_P, and the distance of closest approach between the acceptors and the central axis of the protein is α.

For the Off-Axis model the calculation of the donor fluorescence intensity at any time t after a very short excitation pulse of light as a function of acceptor surface density is given by the expression

$$F(t) = F(0)e^{-t/\tau_D}e^{-\sigma M(t)} \quad \text{(A7)}$$

where $M(t)$ is defined by the following integral

$$M(t) = 2\int_0^{\pi} S(t,\theta)\, d\theta \quad \text{(A8)}$$

$S(t,\theta)$ is given by the integral

$$S(t,\theta) = \int_{r_c(\theta)}^{\infty}(1 - e^{(t/\tau)(R_o/r)^6})r\, dr \quad \text{(A9)}$$

Here

$$r_c(\theta) = [R_p^2 + R_c^2(\theta)]^{1/2} \quad \text{(A10)}$$

where

$$R_c(\theta) = \delta \cos\theta + [\delta^2 \cos^2\theta + (\delta^2 - \alpha^2)]^{1/2} \quad \text{(A11)}$$

For steady-state emission, the ratio of donor fluorescence in the presence over absence of acceptor (I_D/I_{DA}) is given by eq A6 above.

REFERENCES

Adams, P. R. (1981) *J. Membr. Biol. 58*, 161–174.

Albuquerque, E. X., Tsai, M. C., Aronstam, R. S., Witkop, B. Eldefrawi, A. T., & Eldefrawi, M. E. (1980) *Proc. Natl. Acad. Sci. U.S.A. 77*, 1224–1228.

Arias, H. R., Valenzuela, C. F., & Johnson, D. A. (1993a) *J. Biol. Chem. 268*, 6348–6355.

Arias, H. R., Valenzuela, C. F., & Johnson, D. A. (1993b) *Biochemistry 32*, 6237–6242.

Azevedo, J. R., & Johnson, D. A. (1990) *J. Memb. Biol. 118*, 213–224.

Blanton, M. P., & Cohen, J. B. (1992) *Biochemistry 31*, 3738–3750.

Chen, R. F. (1965) *Science 150*, 1593–1595.

Czajkowski, C., & Karlin, A. (1991) *J. Biol. Chem. 266*, 22603–22612.

Czajkowski, C., Kaufmann, C., & Karlin, A. (1993) *Proc. Natl. Acad. Sci. U.S.A. 90*, 6285–6289.

Dreyer, E. B., Hasan, F., Cohen, S. G., & Cohen, J. B. (1986) *J. Biol. Chem. 261*, 13727–13734.

Eldefrawi, M. E., Eldefrawi, A. T., Mansour, N. A., Daly, J. W., Witkop, B., & Albuquerque, E. X. (1978) *Biochemistry 17*, 5474–5483.

Förster, T. (1959) *Discuss. Faraday Soc. 27*, 7–17.

Fung, B. K.-K., & Stryer, L. (1978) *Biochemistry 17*, 5241–5248.

Galzi, J.-L., Revah, F., Bessis, A., & Changeux, J.-P. (1991) *Annu. Rev. Pharmacol. 31*, 37–72.

Haugland, R. P. (1992) *Handbook of Fluorescent Probes and Research Chemicals*, 5th ed., 421 pp, Molecular Probes Inc., Eugene, OR.

Heidmann, T., & Changeux, J.-P. (1979a) *Eur. J. Biochem. 94*, 255–279.

Herz, J. M., & Atherton, S. J. (1992) *Biophys. J. 62*, 74–76.

Herz, J. M., Johnson, D. A., & Taylor, P. (1987) *J. Biol. Chem. 262*, 7238–7247.

Herz, J. M., Johnson, D. A., & Taylor, P. (1989) *J. Biol. Chem. 264*, 12439–12448.

Herz, J. M., Kolb, S. J., Erlinger, T., & Schmid, E. (1991) *J. Biol. Chem. 266*, 16691–16698.

Holowka, D., & Baird, B. (1983) *Biochemistry 22* 3466–3474.

Johnson, D. A., & Yguerabide, J. (1985) *Biophys. J. 48*, 949–955.

Johnson, D. A., Voet, J., & Taylor, P. (1984) *J. Biol. Chem. 259*, 5717–5725.

Johnson, D. A., Cushman, R., & Malekzadeh, R. (1990) *J. Biol. Chem. 265*, 7360–7368.

Johnson, D. A., Leathers, V. L., Martinez, A. M., Walsh, D. A., & Fletcher, W. H. (1993) *Biochemistry 32*, 6402–6410.

Karlin, A. (1991) *Harvey Lect. 85*, 71–107.

Karlin, A. (1993) *Curr. Opin. Neurobiol. 3*, 299–309.

Kistler, J., Stroud, R. M., Klymkowsky, M. W., Lalancette, R. A., & Fairclough, R. H. (1982) *Biophys. J. 37*, 371–383.

Klymkowsky, M. W., & Stroud, R. M. (1979) *J. Mol. Biol. 128*, 319–334.

Krodel, E. K., Beckman, R. A., & Cohen, J. B. (1979) *Mol. Pharmacol. 15* 294–312.

Kubalek, E., Ralston, S., Lindstrom, J., & Unwin, N. (1987) *J. Cell Biol. 105*, 9–18.

Léna, C., & Changeux, J.-P. (1993) *Trends Neurosci. 16*, 181–186.

Marsh, D., & Barrantes, F. J. (1978) *Proc. Natl. Acad. Sci. U.S.A. 75*, 4329–4333.

Neubig, R. R., & Cohen, J. B. (1979) *Biochemistry 18*, 5464–5475.

Olmsted, J., & Kearns, D. R. (1977) *Biochemistry 16*, 3647–3654.

Parker, C. A., & Rees, W. T. (1960) *Analyst 85*, 587–600.

Pedersen, S. E., & Cohen, J. B. (1990) *Proc. Natl. Acad. Sci. U.S.A. 87*, 2785–2789.

Stryer, L., Thomas, D. D., & Carlsen, W. F. (1982) *Methods Enzymol. 81*, 668–678.

Taylor, P., Abramson, S., Johnson, D. A., Valenzuela, C. F., & Herz, J. M. (1991) *Ann. N.Y. Acad. Sci. 265*, 568–587.

Toyoshima, C., & Unwin, N. (1990) *J. Cell Biol. 111*, 2623–2635.

Unwin, N. (1993) *J. Mol. Biol. 229*, 1101–1124.

Valenzuela, C. F., Kerr, J., Duvvuri, P., & Johnson, D. A. (1992a) *Mol. Pharmacol. 41*, 331–336.

Valenzuela, C. F., Kerr, J. A., & Johnson, D. A. (1992b) *J. Biol. Chem. 267*, 8338–8244.

Valenzuela, C. F., Wiegn, P., Yguerabide, J., & Johnson, D. A. (1994) *Biophys. J. 66*, 674–682.

Walkinshaw, M. D., Saenger, W., & Maelicke, A. (1980) *Proc. Natl. Acad. Sci. U.S.A. 77*, 2400–2404.

White, B. H., & Cohen, J. B. (1992) *J. Biol. Chem. 267*, 15770–15783.

Yguerabide, J. (1994) *Biophys. J. 66*, 683–693.

Zingsheim, H. P., Barrantes, F. J., Frank, J., Hänicke, W., & Neugebauer, D.-Ch. (1982) *Nature 299*, 81–84.